Metal supported aluminosilicate ultra-thin films as a versatile tool for studying surface chemistry of zeolites

Shamil Shaikhutdinov* and Hans-Joachim Freund

Abteilung Chemische Physik, Fritz-Haber-Institut der Max-Planck-Gesellschaft,
Faradayweg 4-6, 14195 Berlin, Germany

Abstract

Application of a variety of "surface-science" techniques to elucidate surface structures and mechanisms of chemical reactions at zeolite surfaces have long been considered as almost impossible because of the poor electrical and thermal conductivity of those materials. Here, we show that growth of a thin aluminosilicate film on a metal single crystal under controlled conditions result in adequate and well-defined model systems for zeolite surfaces. In principle, silicate films that contain metals other than Al (e.g. Ti, Fe, etc) may be prepared in a similar way. We believe that this approach opens up a new playground for experimental and theoretical modeling of zeolites, aimed at a fundamental understanding of structure–reactivity relationships in such materials.

Keywords: silica; aluminosilicates, surface structures

* E-mail: shaikhutdinov@fhi-berlin.mpg.de

Introduction

In silicates, Si is coordinated almost exclusively to four oxygen ions forming a [SiO_4] tetrahedron. Although they may exist as isolated SiO_4^{4-} centres, like in olivine $(Fe, Mg)_2SiO_4$, in most cases the silicates are formed by corner-sharing [SiO_4] tetrahedra. Commonly the silicate anions are chains (pyroxenes), double chains (amphiboles), sheets (phyllosilicates, e.g. micas and clays), and three-dimensional frameworks (which are all aluminosilicates, except the quartz and its polymorphs). In aluminosilicates, some of the Si^{4+} ions are replaced by the Al^{3+} ions. The excess negative charge resulted from this replacement is balanced by positive ions, such as H^+ or alkali-metal cations.

Zeolites are microporous members of the aluminosilicate family. As of August 2012, 201 unique zeolite frameworks have been identified, and over 40 naturally occurring zeolite frameworks are known.[1] Even millions of hypothetical zeolite structures have theoretically been predicted based on topological considerations.[2] In zeolites, the [TO_4] (T=Si, Al) tetrahedra, referred to as the primary building units, are arranged into larger structures, called secondary building units (SBU's), which are defined such that the whole framework can be made of only one type of unit repeating in space. Some SBU's are shown in Fig. 1.[1] The simplest SBU's are polygons or (more commonly used term "rings" of different sizes, i.e. n-membered rings (nMR's). Another definition to account for the building blocks of zeolites is the composite building units (CBU's). Some of the most extensively occurring CBU's are the double 4-, 6- and 8-membered rings, outlined in Fig. 1, named *d4r*, *d6r* and *d8r* respectively, according to the CBU's notation.

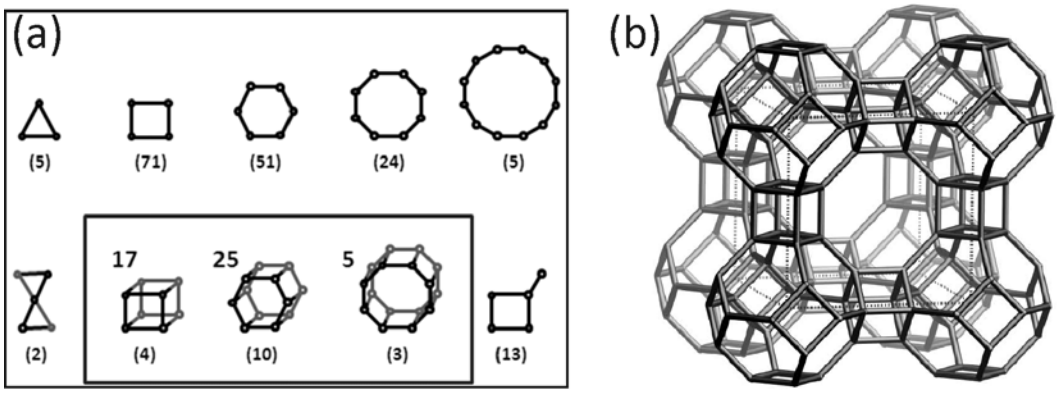

Figure 1. (a) Most frequently observed SBU's shown by connected dots which represent the tetrahedral (Si, Al) atoms. The numbers in parenthesis below each SBU are their frequency of occurrence while the numbers at the upper-left side of the outlined SBUs correspond to the number of zeolite structures in which these units have been found. (b) Linde type A zeolite is shown as an example.[1]

Synthetic zeolites are widely used catalytic materials in the petrochemical industry. The H-form of zeolites is strongly acidic, and as such the zeolites are employed in the acid-base reactions, e.g., isomerisation, alkylation, etc.[3] Regular pore structure of molecular dimensions in zeolites, also known as "molecular sieves", allows selectively sorting molecules and tune selectivity of chemical reactions. The integration of both reaction and separation in the form of zeolite membranes is considered for catalytic membrane reactor applications.

The current understanding of the relation between structure and surface chemistry of silicates and related materials mostly comes from studies employing bulk-sensitive techniques and from theoretical calculations based on educated assumptions about the atomic structures.[3] Application of surface-sensitive techniques to these materials, which are poor electric and thermal conductors, faces severe experimental difficulties. These can, in principle, be overcome by the preparation of a very thin zeolite film on a planar metal substrate, which do not charge upon electron impact or electron emission, and which may quickly be cooled down to liquid nitrogen temperatures. Certainly, the film should exhibit characteristic features of its bulk counterpart. There are, of course, several other attractive features of zeolite thin films that could be utilized for a variety of purposes in such areas as electrochemistry, sensors, photochemistry, etc.

Background

Although numerous preparations of zeolite films of varying magnitude and pore structure have previously been reported,[4] these studies were mostly oriented to membrane applications in catalytic reactors, whereby a zeolite film is supported onto a porous metal or ceramic support. A variety of methods have been used such as dip coating, spin coating, and (to a lesser extent) sputtering, chemical vapor deposition and laser ablation.([4c, 5] and references therein). However, only polycrystalline zeolite films were obtained. In addition, the prepared films were commonly of several hundred's nanometers in thickness to fulfill mechanical stability limitations.

When prepared in the liquid phase, the surface morphology of the zeolite films is determined primarily by the particle size of the zeolite crystallites. A smooth film could therefore be achieved by using the smallest possible zeolite particles, provided by a short synthesis time relative to in situ crystallization. After Martens and co-workers[6] have identified the intermediates formed during the early stages of Silicalite-1 (pure silica zeolite with MFI-type structure) formation, Doyle et al. [7] reported the synthesis of a thin zeolite film supported on Si(100) by spin-coating a solution of Silicalite-1 "precursors" diluted in ethanol, followed by hydration in water vapour and heating to 60°C. The film thickness could be varied by the precursor dilution factor. High resolution transmission electron microscopy (HRTEM) analysis (Fig. 2) and atomic force microscopy (AFM) measurements confirmed that the surface of ~ 2

nm-thick films is smooth over a range of several microns. However, preparation of truly ultra-thin films, i.e. those with thickness of the order of the zeolite unit cell dimension, which show considerable degree of long-range ordering, using "wet chemistry" methods remains challenging.

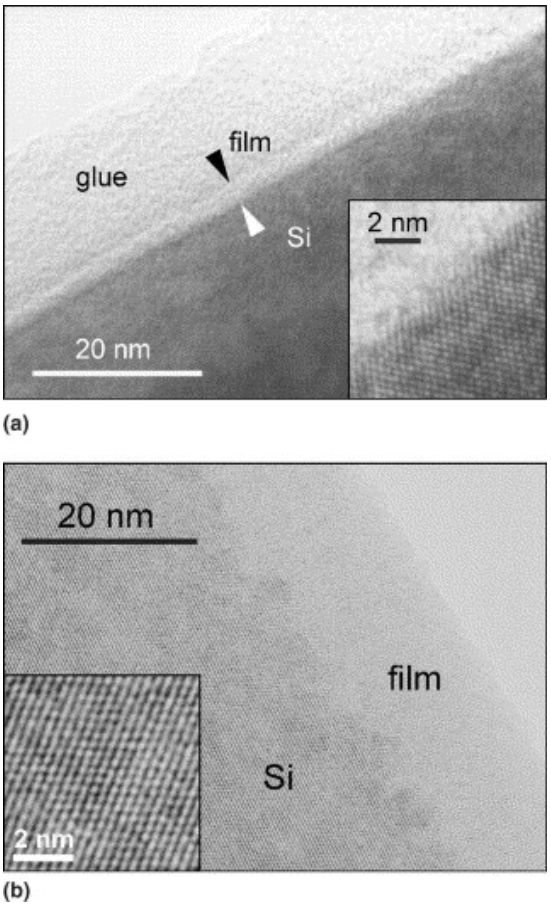

Figure 2. HRTEM cross-section images of 2 nm (a) and 15 nm (b) films. The interface area of film (a) and the atomically resolved substrate of (b) are shown as insets. Reproduced with permission from ref. [7]. Copyright (2003). Elsevier.

It is noteworthy, that HRTEM was also invoked to elucidate the external surface structure of zeolite crystals (see, for example, ref. [8] and references therein). As already mentioned, the nonconducting nature of zeolites precludes the use of scanning tunneling microscopy (STM). (NB: Only one STM study of a zeolite pore structure has been reported, to date.[9] The electrical conductivity has been assigned to the network of hydrogen bonds since the measurements were carried out in air). In principle, AFM enables high resolution imaging of nonconducting surfaces. Recent reviews[10] summarize current progress in this field primarily focused on the elucidation of zeolite growth.

There is another approach, which is the main topic of this Concept, that employs growth of thin silica films using vacuum based deposition methods and its characterization by a variety of "surface science" techniques. Such an approach is currently applied to many transition metal oxides (see, for example, refs.[11]). Once prepared and analyzed at the atomic level, the aluminosilicate films could then be used for elucidating mechanisms of chemical reactions on zeolites.

The first ever preparation of "surface science" models of zeolites, to the best of our knowledge, should be referred to the work of Somorjai and co-workers[12], who grew thin films (< 10 nm) of silica-alumina by argon ion beam sputter deposition on gold foil using different HY-zeolites as targets. Structural characterization was performed with x-ray photoelectron spectroscopy (XPS), scanning electron microscopy, x-ray diffraction and scanning Auger electron spectroscopy (AES). The prepared thin films appeared homogeneous, but amorphous. The films showed some acitivity in cumene cracking at 570 K, whereas thin films prepared from alumina or silica targets or a mixture of the two were inactive.

Goodman and co-workers[13] prepared mixed Al_2O_3/SiO_2 thin films by low temperature deposition of metallic Al onto a amorphous SiO_2 film, grown on a Mo(100) substrate, and annealing in ultrahigh vacuum (UHV). In the temperature regime from 100 to 800 K, Al was completely oxidized and metallic Si is formed. In the temperature range from 800 to 1200 K, the formation of Si-O-Al bonds probably occurred via the concerted diffusion of aluminum oxide into the bulk of the SiO_2 film with the concomitant desorption of volatile silicon monoxide as a result of the solid state reaction of Si and SiO_2. An XPS study indicated that the electronic structure of these films were very similar to that of bulk aluminosilicates. Due to the absence of water during the preparation, surface hydroxyl groups were not formed. The authors also mentioned that preparation of a mixed oxide film by co-deposition of Al and Si in an oxygen environment led to the deposition of a less than uniform film.

In the following sections, we demonstrate the preparation of well-defined silicate thin films on metal single crystals. The films exhibit sheet-like morphology and can be doped with Al, ultimately resulting in the aluminosilicate films. When prepared on a proper metal substrate, the aluminosilcate films become adequate model systems for zeolite surfaces: the films (i) are only weakly bound to the underlying metal support; (ii) are constituted of tetrahedral [SiO_4] and [AlO_4] units; and (iii) expose acidic OH species. We believe that this approach opens up an avenue for experimental and theoretical modeling of zeolite surfaces aimed at a fundamental understanding of structure-reactivity relationships on such materials.

Ultra-thin pure silicate films on metals

To date, preparation of thin silica films on metal single crystals has been reported for Mo(100), Mo(110), Mo(112), Ni(111), Pd(100), Ru(0001) and Pt(111) ([14] and references

therein). The preparation commonly includes physical vapor deposition of Si in vacuum or in oxygen ambient (ca. 10^{-7} mbar) and subsequent annealing in UHV or oxygen at high temperatures. Among the systems studied, only ultra-thin films grown on Mo(112) and Ru(0001) can be considered as structurally identified. By a combination of low energy electron diffraction (LEED), infrared reflection-absorption spectroscopy (IRAS), STM, XPS, and density functional theory (DFT) calculations, it was shown that ultra-thin films on Mo(112)[15] and Ru(0001)[16] consist of a single layer of corner sharing [SiO_4] tetrahedra (schematically shown in Fig. 3a), resulting in a $SiO_{2.5}$ composition. In these so-called "monolayer" films, one of oxygen atoms of each [SiO_4] is bonded to the metal atoms. In addition, silica films on Ru(0001) may form a "bilayer" structure, where two $SiO_{2.5}$ monolayers are linked through the bridging oxygen layer as a mirror plane (see Fig. 3b). This bilayer film is fully saturated with oxygen on either side and weakly bound to underlying Ru(0001) by dispersion forces.[17] In contrast to monolayer films, the bilayer films exist in both, crystalline and amorphous states (see Figs. 3(b,c)).[18]

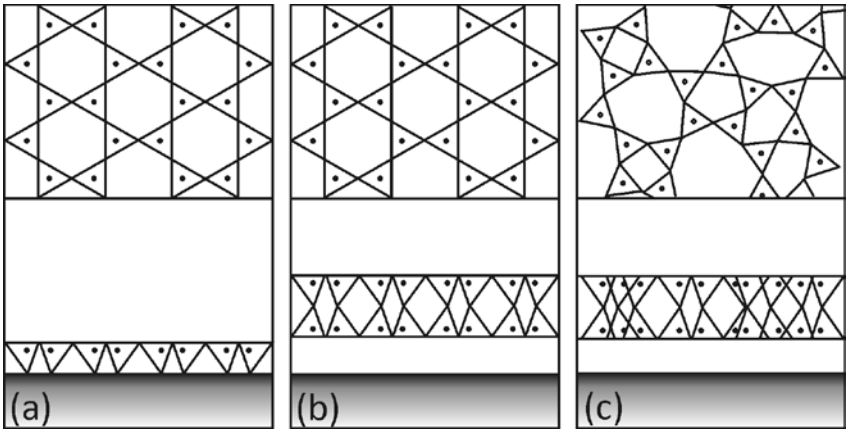

Figure 3. Schematic representations of ultra-thin silica thin films grown on metal single crystal surfaces. Top and cross-sectional views of monolayer $SiO_{2.5}$ films (a), and bilayer SiO_2 films in the crystalline (b) and disordered (c) states. All structures are formed by corner-sharing [SiO_4] tetrahedra. Only the positions of Si are marked by dots for clarity.

Attempts to further grow the silica films in a layer-by-layer layer mode on both, Mo and Ru supports resulted only in silica overlayers structurally identical to the vitreous silica films grown on Si wafers. The principal structure of the thin silica films can be identified by IRAS as illustrated in Fig. 4. The asymmetric stretching vibrations of the Si-O-Mo(Ru) linkages falls into the region 1050 - 1150 cm^{-1}. Meanwhile, bilayer films (both, crystalline and vitreous) are characterized by the sharp band at ~1300 cm^{-1}, assigned to the asymmetric stretching of the Si-O-Si linkage between two monolayers. The band at 1257 cm^{-1} with a prominent shoulder at 1164 cm^{-1}, developed for the multilayer films on any metal support, is well-documented for the bulk-like silica (e.g., quartz).[14] It therefore appears that films thicker than bilayer exhibit a three-dimensional network of [SiO_4] tetrahedra rather than the layered structure observed for

mono- and bi-layer films. These “thick” films exhibit smooth surfaces, with a corrugation amplitude of ca. ~1 Å as measured by STM.

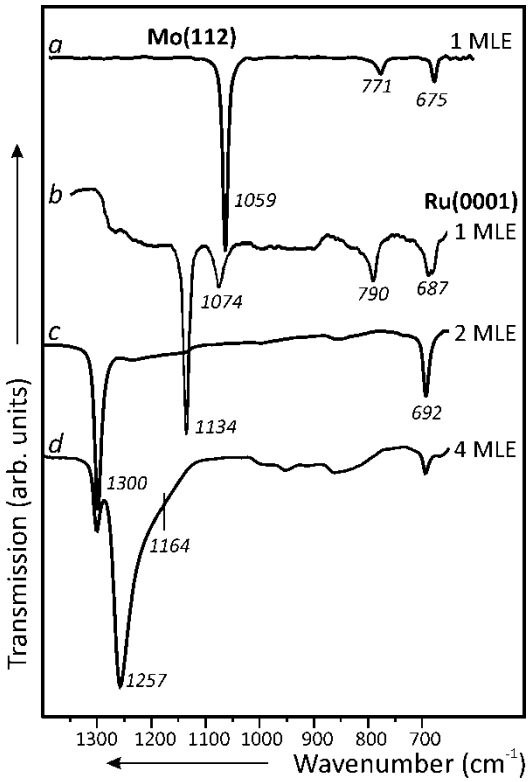

Figure 4. IRAS spectra of ultrathin silica films grown on metal single crystals. The nominal film thickness is indicated in monolayers equivalent (MLE) such that 1 MLE corresponds to a closed monolayer film. (a) $SiO_{2.5}$/Mo(112); (b) $SiO_{2.5}$/Ru(0001); (c,d) SiO_2/Ru(0001).

Interestingly, no monolayer, but amorphous bilayer films were only observed on Pt(111).[19] The support effect for the structure of the films (monolayer vs bilayer) can be rationalized on the basis of the metal-oxygen bond strength, which is considerably different for the Mo, Ru and Pt supports studied. The bond is very strong in the SiO-Mo linkage, that favors the monolayer structure on Mo(112), whereas on Pt(111) silica forms only bilayer structure. Ru(0001) exhibits the intermediate properties and forms both mono- and bi-layer structures.

Aluminosilicate thin films

The crystalline silica films on Mo(112) have been utilized as a template to prepare aluminosilicate films. However, the preparation involving Al deposition onto the preformed $SiO_{2.5}$/Mo(112) film and subsequent annealing led to film disordering as judged by LEED. Also STM inspection of the resulted films revealed a rough and heterogeneous surface. In order to

facilitate the intermixing of aluminum and silicon atoms in the film, Al and Si were co-deposited onto an O-precovered Mo(112) surface in an oxygen ambient followed by high temperature annealing at ~ 1100 K. This approach turned out to be successful.[20]

The films at relatively low Al/Si ratios (< 0.2) showed a sharp c(2×2)-Mo(112) LEED pattern as in the pure silica film. XPS spectra revealed the silicon and aluminum atoms in the fully oxidized states. IRAS spectra became broader and underwent red-shifts by ~ 30 cm^{-1}. STM images showed atomically flat terraces (Fig. 5a) with basically the same honeycomb structure as observed for the pure silica films. However, numerous additional bright spots were observed, whose density correlated well with the aluminum content in the film and as such they were assigned to Al-related species. The random distribution of these spots implies a random distribution of the Al atoms in the film.

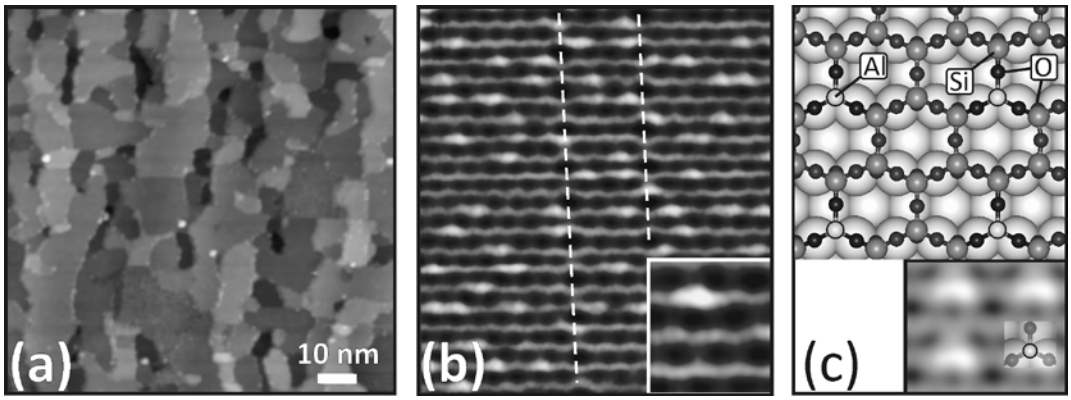

Figure 5. (a,b) Large scale and high-resolution STM images of an aluminosilicate (Al:Si ~ 1:5) monolayer film prepared on Mo(112). The honeycomb-like morphology corresponds to the structure depicted in Fig. 3a. The white dashed lines in (b) indicate anitiphase domain boundaries consisiting of a row of 8- and 4-membered rings (also present in pure silica films). The inset zooms in asymmetric bright protrusions, randomly distributed at the surface. (c) Top view of the structural (periodic) model,[20] where Al substitutes Si in the silica framework, but has no bond to the Mo surface. Inset shows STM simulation to compare with the high-resolution STM image shown in (b).

These results suggested that the aluminosilicate film on Mo(112) consists of a monolayer of corner-sharing [SiO_4] tetrahedra, in which some Si^{4+} ions are replaced by Al. In the aluminosilicate minerals, the charge imbalance introduced by the Al^{3+} ions is compensated by the intercalation of H^+ or alkali-metal cations. Since alkali metals were not present during the film preparation, and H^+ ions were not detected by vibrational and electron spectroscopy, the extra charge in thin films is most likely compensated by the metal substrate. In this AlO_4-model, the Al^{3+} ions are each coordinated to four O^{2-} ions in the same geometry as the Si^{4+} ions in the pure silica film. Another possibility includes the Al^{3+} ions only coordinated to three O^{2-} ions in the topmost layer, thus resulting in a AlO_3-model depicted in Fig. 5c. Based on DFT calculations, both structures were stable with nearly equal energies. However, STM image simulations

clearly favored the AlO_3 model (compare insets in Figs. 5(b,c)). This model also fits the results of high resolution XPS studies performed with synchrotron radiation.

Certainly, for the monolayer aluminosilicate films, a metal support has to be explicitly involved in a proper description of the systems electronic structure, which definitely limits their use as an adequate model of zeolitic surfaces. Indeed, such films lack the negative framework charge present in zeolites as well as acidic Si-OH-Al species. Since bilayer silica films on Ru(0001)[17] are only weakly bound to the underlying metal support, it was near at hand to try to incorporate Al into these films.[21] The preparation includes Si and Al co-deposition in total amounts equal to the amount of Si necessary to prepare a SiO_2 bilayer film. XPS measurements allowed to determine the average film composition and showed both Si and Al in the highest oxidation states. The surfaces show a (2×2)-Ru(0001) LEED pattern, suggesting a high degree of crystallinity. With increasing Al content, the principal phonon band at 1300 cm^{-1} only gradually red-shifts to ~1280 cm^{-1} (Fig. 6c) without losing intensity, thus indicating that the films essentially retain the bilayer structure as of pure silicate films.

An STM study revealed atomically flat surfaces of the films. At low Ai:Si atomic ratios, areas (labeled A in Fig. 6a) showing a hexagonal lattice of protrusions were observed which exhibited a considerably higher corrugation amplitude as compared to the rest of the surface (labeled B), which in turn exposed a surface virtually identical to that of crystalline SiO_2 films. The surface area covered by the A domains correlated with the Al:Si ratio, thus suggesting that the Al atoms are not randomly distributed across the surface, as it was found for a monolayer aluminosilicate film on Mo(112) (see Fig. 5b), but segregate into domains. This finding is not trivial in its own right, since it is commonly accepted, based on electrostatic considerations, that the Al atoms arrange in zeolites as far as possible from each other.[22] As a possible explanation for this effect can be the lattice strain, induced by the Al incorporation into the silicate frame, which can be minimized if Al-containing species locate near each other as theoretically predicted.[23] Another explanation could be related to the possible inhomogeneity of Al and Si species at the deposition step, i.e. before film annealing at high temperatures. Note also, that although STM images allow the determination of the position of tetrahedral atoms, the distinction between Al and Si atoms is not resolved yet. This issue is studied at present.

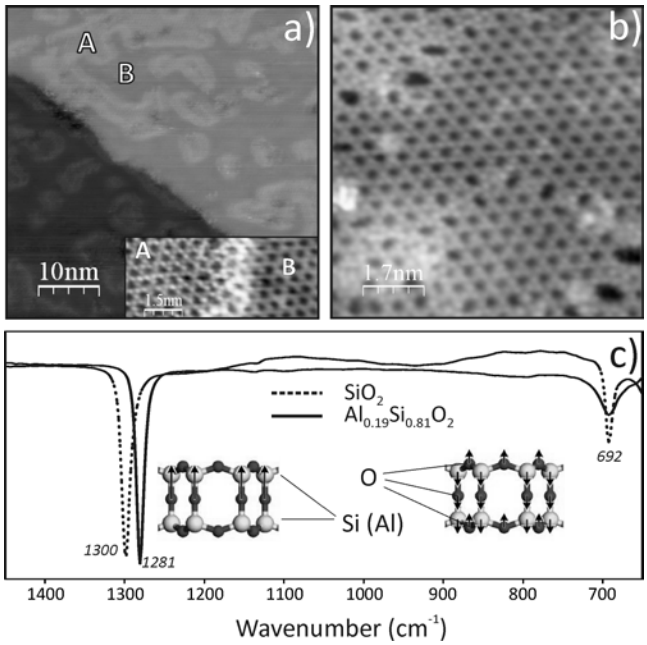

Figure 6. (a) STM image of an $Al_{0.12}Si_{0.88}O_2$ film on Ru(0001). Domains A show higher corrugation amplitude as compared to domains B, which in turn show the same morphology as all-SI silicate crystalline films. (b) STM image of an $Al_{0.36}Si_{0.64}O_2$ film showing a rather uniform surface, where domains A and B can hardly be discriminated. (c) IRAS spectra of a pristine SiO_2 film (dashed line) and an $Al_{0.19}Si_{0.81}O_2$ film (solid line). The respective vibrational modes are schematically shown.

The surface coverage measured by STM of Al containing domains A[21] was consistent with the estimations based on that (i) Al first populates the bottom cation layer, which is closer to the metal substrate, to overcome charge balance issues (very recent studies comprising XPS measurements at grazing and normal electron emissions proved this scenario);[24] and (ii) the Al distribution within the bottom layer follows the Lowenstein's rule,[25] stating that Al-O-Al linkages in zeolitic frameworks are forbidden. Following the same rule, Al must occupy sites in the upper cation layer at the Al:Si ratios above 0.5. Indeed, such films showed a rather uniform surface in STM (domains A were not distinguishable anymore), albeit the surface exposed both crystalline and disordered phases, as shown in Fig. 6b.

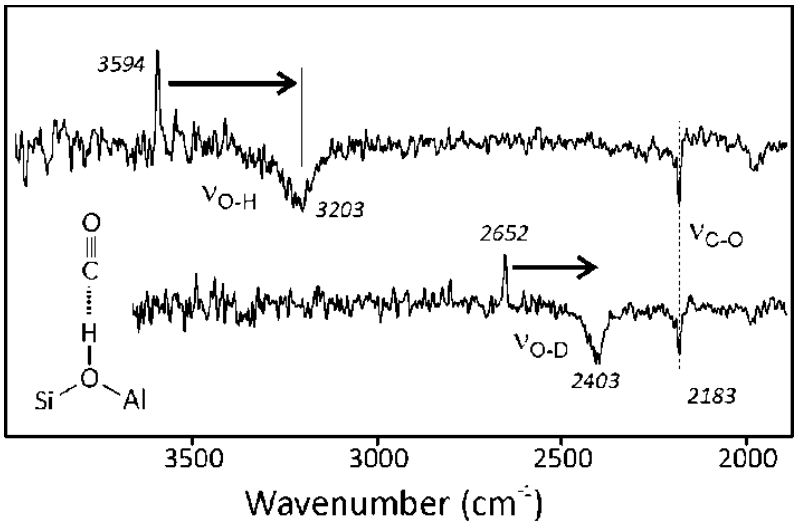

Figure 7. IRAS spectra of the $Al_{0.4}Si_{0.6}O_2$ films exposing OH (top spectrum) and OD (bottom spectrum) recorded in 2 × 10^{-5} mbar of CO.[21] Each spectrum was divided by a reference spectrum taken before CO exposure. The formation of CO…HO adduct that causes ν(OH) and ν(CO) bands shift is schematically shown.

The "as prepared" films did not show any IRAS detectable OH species. Exposure to water vapor (typically, ~ 10^{-6} mbar) at room temperature did not result in hydroxyl groups, either. To form surface OH species, the aluminosilicate films had to be exposed to water at ~ 100 K, resulting in an amorphous solid water (ice) overlayer. The film was then heated to 300 K to desorb weakly bound water molecules monitored by mass spectrometry.

IRAS measurements showed a sharp signal at 3594 cm^{-1}, which falls in the frequency range of the hydroxyl groups in the bridging Si-OH_{br}-Al positions in zeolites.[26] For comparison, only silanol (Si-OH) groups with a characteristic OH vibration (ν_{O-H}) at 3750 cm^{-1} were observed on pure silicate films. The fact, that OH_{br} species only appeared at high Al/Si ratios, is consistent with the sequential population of Al first in the bottom and then in the top cation layer. The bridging OH_{br} groups are thermally stable up to ~ 650 K.

Once formed OH groups can be replaced by OD upon exposure to D_2O at ~ 100 K and heating to 300 K.[21] The OH_{br} signal at 3594 cm^{-1} disappears, and the OD_{br} signal appears at 2652 cm^{-1}, thus indicating H/D exchange reaction, which is a well-known phenomenon in zeolite chemistry.

The acidity of zeolites can be measured by adsorption of CO as a weak base,[27] which binds to the acidic proton through the C atom to form an CO···HO adduct. This induces a red-shift in ν(OH) and a blue-shift of ν(CO) (compared to a gas phase 2143 cm^{-1}), and the magnitude of the shift is proportional to the degree of acidity.[27-28] The IRAS measurements on $Al_{0.4}Si_{0.6}O_2$ films revealed the red-shift about 379 and 243 cm^{-1}, for ν(OH) and ν(OD), and the blue-shift of 40 cm^{-1} for ν(CO), respectively (see Fig. 7). These results indicate that the acidity of the OH species formed on the aluminosilicate films at high Al/Si ratios is among the highest ones

reported for zeolites. For comparison, in zeolite H-SSZ-13, a high silica form of chabasite, the ν(OH) red-shifts by 316 cm^{-1} and ν(CO) blue-shifts by 38 cm^{-1}. [26]

Therefore, the characteristics of the metal supported aluminosilicate films possessing Si-OH-Al surface species perfectly fit into what is known about regular zeolites. The films expose strongly acidic sites and exhibit H–D exchange reaction. These well-defined films constitute the first well-defined model system where the surface properties of zeolites can be modeled by a surface-science approach.

Two-dimensional films versus Three-dimensional frameworks

Certainly, the planar aluminosilicate films cannot directly address the properties of zeolites related to their pore structures. However, the possibility to visualize the atomic structure of such films with STM may also aid in a deeper understating of the mechanism by which the frameworks are assembled, which is currently a topic under active debate.[29] This and related issues were recently addressed by Boscoboinik et al.[30] who have performed quantitative STM analysis of the prepared films. The results revealed some interesting topological relations between two-dimensional films and zeolites.

As schematically shown in Figs. 3(b,c) (see also inset in Fig. 6c) the bilayer silicate films consist of a sheet of double *N*-membered rings. Figure 6 clearly shows that the most abundant structure in the aluminosilicate films is the *d6r* which is zoomed in Fig. 8a. In addition, there were few other structures observed by STM, some of those are depicted in Figs. 8(b,c) together with its schematic representations. In most cases, 5-membered rings (5MR) are located next to 7MR, while 4MR are located next to 8MR (or larger rings). The ring size distribution for the surface regions out of the domains exhibiting exclusively 6MRs is displayed in Fig. 8d. The histogram reveals a rather broad distribution between N = 4 and 8. For comparison, the results for the vitreous silica films[18a] are also shown. This distribution has a peak at 6MR, and 5MR and 7MR being the next most abundant species, with negligible amounts of 4MRs. The lack of the 4MR was also observed in the recent study using HRTEM.[31] In principle, the presence of adjacent 5- and 7MRs can easily be explained as a result of “disproportionation” of the two 6MRs, which most likely accounts for their observation in both systems.

However, in the case of aluminosilicate films, the population of 4MR and 8MR is significantly higher than in the vitreous silica films and is comparable to the number of 5MR and 7MR. Therefore, the increase in the number of 4- and 8MRs can be clearly attributed to the incorporation of Al atoms into the framework. This finding is in a good agreement with the fact that zeolites show a strong preference for ring sizes having even numbers of tetrahedral atoms. The latter is basically the consequence of the Lowenstein’s rule, which leads to the formation of Al—O—Si moieties which repeat around the rings, ultimately resulting in the even-numbered

rings. Apparently, Al incorporation results in a more flexible network as compared to all-Si silicalites.

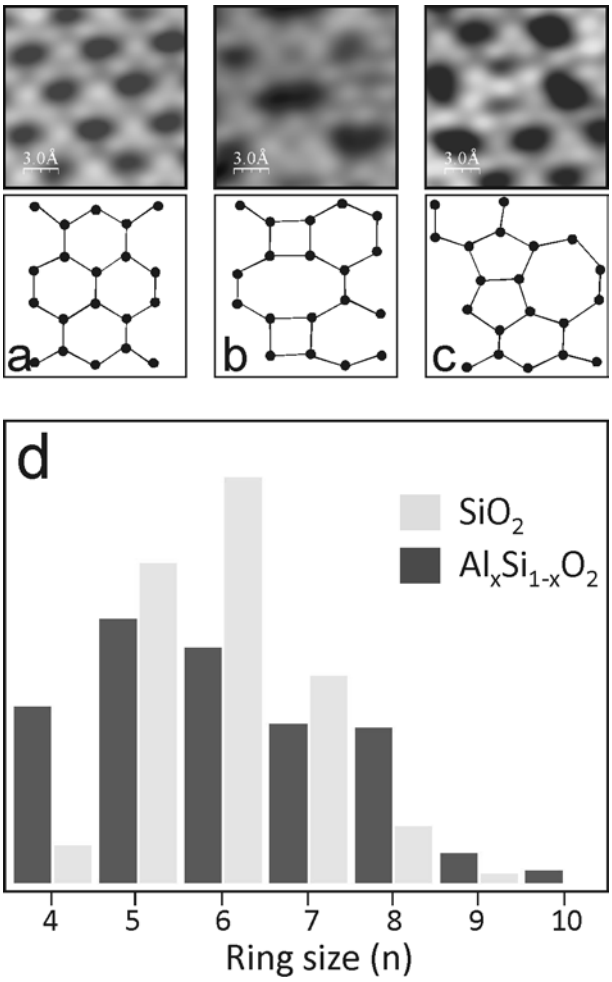

Figure 8. (a-c) Close-ups of STM images and its schematic representations, showing several rings structures on aluminosilicate films. (d) Ring size distribution derived from atomically resolved STM images. Note, that the ordered regions dominating the film surface (see Fig. 6b) were not taken into account. The distribution observed for vitreous silica films in ref. [18a] is shown for comparison.

Moreover, it has turned out that the arrangement of alternating 4-, and 8MRs surrounded by 6MRs in the films resembles the planar structures artificially created by unfolding of the rings forming the α-cage in LTA-type zeolites (see details in ref.[30]). This finding may, for example, shed light on the mechanism of the thermal transformation of Ba^{2+} substituted zeolite A into the layered barium aluminosilicate (hexacelsian).[32]

Concluding remarks

This short review shows that the ultrathin silicate and aluminosilicate films open a new playground for experimental and theoretical modeling of zeolites, aimed at a fundamental understanding of structure–reactivity relationships in these materials. Furthermore, in a similar way one could prepare films containing metal cations other than Al, such as Titanium Silicalite (TS-1), which is a crystalline zeotype material, in which tetrahedral [TiO_4] and [SiO_4] units are arranged in a MFI structure. Another candidate would be Fe-containing zeolites like Fe-ZSM5, which were suggested as efficient oxidation catalysts.[33] The fabrication of well-ordered films with three-dimensional structures is the next step in this approach. If successful, this will allow one to study also molecular sieve properties of zeolites and porosity-related effects on reactivity of such materials.

Acknowledgements

We thank all our past and present co-workers, whose names appear in the cited papers, for their tremendous work in the laboratories. We acknowledge fruitful collaboration with J. Sauer and his group at the Humboldt University at Berlin. The work has been supported by Fonds der Chemischen Industrie and Deutsche Forschungsgemeinschaft.

References

[1] *Atlas of Zeolite Framework Types*, 6-th ed., Elsevier, **2007**.

[2] M. D. Foster, M. M. J. Treacy. *A Database of Hypothetical Zeolite Structures*. Available from: http://www.hypotheticalzeolites.net.

[3] *Zeolites and Catalysis: Synthesis, Reactions and Applications*, (Eds. J. Cejka, A. Corma, and S. Zones), **2010**, Weinheim: Wiley-VCH.

[4] a) A. S. T. Chiang, K.-j. Chao, *Journal of Physics and Chemistry of Solids* **2001**, *62*, 1899-1910; b)M. Tsapatsis, *Science* **2011**, *334*, 767-768; c) E. E. McLeary, J. C. Jansen, F. Kapteijn, *Microporous and Mesoporous Materials* **2006**, *90*, 198-220.

[5] S. P. Davis, E. V. R. Borgstedt, S. L. Suib, *Chemistry of Materials* **1990**, *2*, 712-719.

[6] C. E. A. Kirschhock, V. Buschmann, S. Kremer, R. Ravishankar, C. J. Y. Houssin, B. L. Mojet, R. A. van Santen, P. J. Grobet, P. A. Jacobs, J. A. Martens, *Angewandte Chemie International Edition* **2001**, *40*, 2637-2640.

[7] A. M. Doyle, G. Rupprechter, N. Pfänder, R. Schlögl, C. E. A. Kirschhock, J. A. Martens, H. J. Freund, *Chemical Physics Letters* **2003**, *382*, 404-409.

[8] I. Díaz, E. Kokkoli, O. Terasaki, M. Tsapatsis, *Chemistry of Materials* **2004**, *16*, 5226-5232.

[9] J. C. Jansen, J. Schoonman, H. van Bekkum, V. Pinet, *Zeolites* **1991**, *11*, 306-307.

[10] a) M. W. Anderson, J. R. Agger, N. Hanif, O. Terasaki, T. Ohsuna, *Solid State Sciences* **2001**, *3*, 809-819; b) M. W. Anderson, *Current Opinion in Solid State and Materials Science* **2001**, *5*, 407-415; c) J. R. Agger, N. Hanif, C. S. Cundy, A. P. Wade, S. Dennison, P. A. Rawlinson, M. W. Anderson, *Journal of the American Chemical Society* **2002**, *125*, 830-839.

[11] a) H. Kuhlenbeck, S. Shaikhutdinov, H.-J. Freund, *Chemical Reviews*, accepted; b) S. A. Chambers, *Surface Science Reports* **2000**, *39*, 105-180; c) W. Weiss, W. Ranke, *Progress in Surface Science* **2002**, *70*, 1-151.
[12] I. Böszörményi, T. Nakayama, B. McIntyre, G. A. Somorjai, *Catalysis Letters* **1991**, *10*, 343-355.
[13] C. Gründling, J. A. Lercher, D. W. Goodman, *Surface Science* **1994**, *318*, 97-103.
[14] S. Shaikhutdinov, H.-J. Freund, *Advanced Materials*, accepted.
[15] J. Weissenrieder, S. Kaya, J.-L. Lu, H.-J. Gao, S. Shaikhutdinov, H.-J. Freund, M. Sierka, T. K. Todorova, J. Sauer, *Physical Review Letters* **2005**, *95*, 076103.
[16] B. Yang, W. E. Kaden, X. Yu, J. A. Boscoboinik, Y. Martynova, L. Lichtenstein, M. Heyde, M. Sterrer, R. Wlodarczyk, M. Sierka, J. Sauer, S. Shaikhutdinov, H.-J. Freund, *Physical Chemistry Chemical Physics* **2012**, 14, 11344 - 11351.
[17] D. Loeffler, J. J. Uhlrich, M. Baron, B. Yang, X. Yu, L. Lichtenstein, L. Heinke, C. Büchner, M. Heyde, S. Shaikhutdinov, H. J. Freund, R. Wlstrokodarczyk, M. Sierka, J. Sauer, *Physical Review Letters* **2010**, *105*, 146104.
[18] a) L. Lichtenstein, C. Büchner, B. Yang, S. Shaikhutdinov, M. Heyde, M. Sierka, R. Włodarczyk, J. Sauer, H.-J. Freund, *Angewandte Chemie International Edition* **2012**, *51*, 404-407; b) M. Heyde, S. Shaikhutdinov, H.-J. Freund, *Chemical Physics Letters* **2012**, 550, 1-7.
[19] X. Yu, B. Yang, J. A. Boscoboinik, S. Shaikhutdinov, H.-J. Freund, *Applied Physics Letters* **2012**, *100*, 151608-151604.
[20] D. Stacchiola, S. Kaya, J. Weissenrieder, H. Kuhlenbeck, S. Shaikhutdinov, H.-J. Freund, M. Sierka, T. K. Todorova, J. Sauer, *Angewandte Chemie International Edition* **2006**, *45*, 7636-7639.
[21] J. A. Boscoboinik, X. Yu, B. Yang, F. D. Fischer, R. Włodarczyk, M. Sierka, S. Shaikhutdinov, J. Sauer, H.-J. Freund, *Angewandte Chemie International Edition* **2012**, *51*, 6005-6008.
[22] E. Dempsey, *J. Catal.* **1974**, *33*, 497-499.
[23] K. P. Schroder, J. C. Sauer, *J. Phys. Chem.* **1993**, *97*, 6579-6581.
[24] J. A. Boscoboinik, B. Yang, X. Yu, B. Liu, S. Shaikhutdinov, H. J. Freund, *unpublished.*
[25] W. Loewenstein, *Am. Miner.* **1954**, *39*, 92-96.
[26] S. Bordiga, L. Regli, D. Cocina, C. Lamberti, M. Bjørgen, K. P. Lillerud, *The Journal of Physical Chemistry B* **2005**, *109*, 2779-2784.
[27] A. Zecchina, C. Lamberti, S. Bordiga, *Catalysis Today* **1998**, *41*, 169-177.
[28] G. Busca, *Catalysis Today* **1998**, *41*, 191-206.
[29] C. S. Cundy, P. A. Cox, *Microporous and Mesoporous Materials* **2005**, *82*, 1-78.
[30] J. A. Boscoboinik, X. Yu, B. Yang, S. Shaikhutdinov, H. J. Freund, *Microporous and Mesoporous Materials* **2012**, 165, 158 - 162
[31] P. Y. Huang, S. Kurasch, A. Srivastava, V. Skakalova, J. Kotakoski, A. V. Krasheninnikov, R. Hovden, Q. Mao, J. C. Meyer, J. Smet, D. A. Muller, U. Kaiser, *Nano Letters* **2012**, *12*, 1081-1086.
[32] J. Djordjevic, V. Dondur, R. Dimitrijevic, A. Kremenovic, *Physical Chemistry Chemical Physics* **2001**, *3*, 1560-1565.
[33] G. I. Panov, *CATTECH* **2000**, *4*, 18-31.